Direct observation of remanent magnetic states in epitaxial fcc Co small disks

C. A. F. Vaz, L. Lopez-Diaz, M. Kläui, and J. A. C. Bland*

Cavendish Laboratory, University of Cambridge, Cambridge, CB3 0HE, U. K.

T. L. Monchesky and J. Unguris

National Institute of Standards and Technology,

100 Bureau Drive Stop 8412, Gaithersburg, MD 20899-8412, U.S.A.

Z. Cui

Rutherford Appleton Laboratory, Chilton, Didcot OX11 0QX, U. K.

(Dated: November 20, 2002)

Abstract

The magnetic nanostructure of epitaxial fcc Co/Cu(001) circular elements ($\sim$1.7 μm in diameter) has been imaged with scanning electron microscopy with polarisation analysis (SEMPA). The disks are obtained by ultrahigh vacuum deposition of the metal films onto a pre-patterned Si(001) substrate. The structures are high enough (height 700 nm) to ensure that the continuous background film and that of the circular structures are not physically connected. A closed flux configuration (a quadrant configuration) is observed for some of the disks, characteristic of systems with cubic anisotropy. The measured width of the 90$^{\rm o}$ domain wall varies from 70 ± 25 nm close to the vortex core, up to 150 ± 25 nm at a normalised distance $r/r_d \approx 0.625$ from the vortex core (where r_d is the domain wall length from the vortex core to the disk periphery), i.e., significantly exceeding the bulk domain wall width, and increasing further with increasing distance from the vortex core. Such a wide domain wall is a consequence of the geometrical constraints imposed by the element, thus defining a geometrically constrained domain wall. This view is supported by detailed micromagnetic simulations which also show that the domain wall width increases dramatically with radial position from the disk centre.

PACS numbers: PACS:75.60.Ch, 75.25.+z, 75.40.Mg, 75.70.-i

I. INTRODUCTION

Small magnetic elements have received considerable attention recently, in large measure due to their potential for memory elements in high density storage media or as miniaturised sensor elements,[1] but also because they have opened a new field of research with its specific problems and dedicated experimental techniques. Of particular interest is the study of the equilibrium magnetic states and magnetisation reversal mechanisms in small elements, which are strongly determined by the interplay of the different anisotropy terms with the physical shape of the element. In fact, the shape of the element so fundamentally influences the switching behaviour of the magnetisation, that a large effort has been spent with the purpose of finding the geometry that provides the simplest, fastest and most reproducible switching mechanism, which are essential prerequisites for device applications.[1–6] As a striking example of the influence of the shape in the equilibrium magnetic state, it is observed that micrometer sized NiFe circular elements show a circular magnetisation state (vortex state)[7] while square elements show a domain state that resembles the Landau-Lifshitz (quadrant) domain structure.[8] In both cases the magnetostatic energy is minimised by flux closure commensurate with the element geometry. No extra cost arrives from the anisotropy term, which in NiFe is negligible compared with the magnetostatic energy term, but for other materials the effect of the anisotropy is expected to play an important role in determining the equilibrium magnetic states and ultimately the reversal of the magnetisation process. In fact, the role of the magnetic anisotropy has not been so extensively investigated, although some studies have used epitaxial systems such as fcc Co(001),[2,9] hcp Co(0001),[10] bcc Fe(001) and bcc Fe(110).[11] In general, the effect of the magnetic anisotropy is to restrict the states with flux closure to those compatible with local domains pointing along the easy direction axis. In disks, materials with cubic anisotropy form quadrant structures, and materials with uniaxial anisotropy have a multidomain state with parallel magnetic domains[11]. Ring structures, in contrast, show local domain-like features when a cubic anisotropy is present.[12,13] Less clear, however, is how the magnetocrystalline anisotropy and the dipolar interactions (i.e., shape of the element) together determine the form and extent of the effective transition at a magnetic domain boundary in small elements. More generally, there is strong current interest in the concept of a geometrically constrained domain wall.[14]

In this article we use scanning electron microscopy with polarisation analysis (SEMPA)

to study the remanent states in micrometer size fcc Co(001) disks epitaxially grown on Cu(001). In particular, we look into the details of the domain wall between the observed magnetic domains to show that it is strongly constrained by both the shape of the element and the magnetic anisotropy. The SEMPA technique has the advantage of not influencing the magnetic state of the sample, unlike more invasive techniques, such as, magnetic force microscopy (MFM).[15] In addition, Co thin films deposited on Cu(001) have been extensively studied[16–20] and provide a well characterised system, ideal for the study of magnetic elements.

II. RESULTS AND DISCUSSION

The elements studied here were fabricated by deposition onto a prepatterned Si(001) substrate. A mask consisting of an array of disks and rings was first defined on the resist layer by electron beam lithography and the unprotected Si was etched down by reactive ion etching. In this paper, we consider only the magnetic characterisation of the disk elements.[12,13] The disk diameter was fixed at $\sim$1.7 μm and the separation between the elements was set to 6 μm. This assures that the disks do not interact with each other. Before film deposition, the Si prepatterned substrate was etched in a 10% HF solution and loaded into the MBE chamber (base pressure $\sim 3 \times 10^{-10}$ mbar). A 100 nm Cu(001) template layer was first deposited onto the Si(001) onto which a 34 nm Co layer was deposited [Co grows epitaxially in the fcc phase on the Cu(001) surface[17]]. A thin 2 nm Cu layer was then deposited and this trilayer was finally capped with a 4 nm Au layer to prevent oxidation of the structure. The height of the Si structures (700 nm) ensures that the continuous background film and that of the circular structures are not physically connected. A top view scanning electron microscopy (SEM) image of some of the disks is shown in Fig. 1(a). In contrast to conventional lithography by lift-off of the magnetic film, this alternative method has the possibility of achieving much smaller structures and protects the magnetic film from contamination during the lithographic process, therefore minimising unwanted changes in its magnetic properties. As a drawback, the structure is left with a continuous background magnetic layer. This film can, however, be disconnected from the disk by making the height of the mesas tall enough. This method was previously shown to yield successful results for ring elements,[2,9,21] where a stable bi-domain state was observed at remanence.

The magnetic domain structure of the elements was imaged at remanence with SEMPA. A

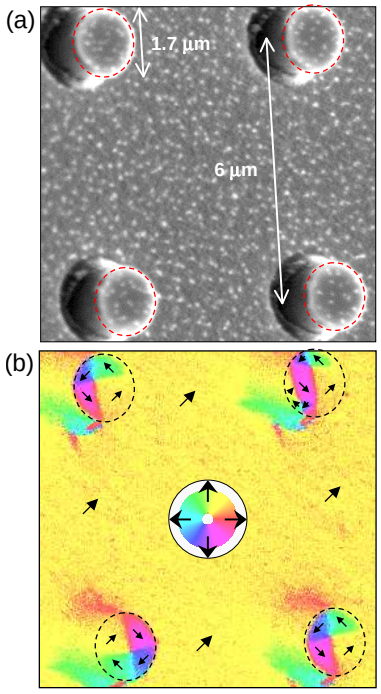

FIG. 1: SEMPA images of four disks: (a) topography of the disks showing the nanopillars rising well above the background, clearly separating the magnetic material deposited in the trenches from that on the mesas. (b) Magnetisation direction. Because of the measurement geometry, the magnetisation data just to the left of the disk is in the shadow of the detector and should be ignored. Superimposed circles and arrows are guides to the eye. The inset shows the key to the orientation of the magnetisation.

detailed description of this technique can be found elsewhere.[22] The sample is introduced into a UHV chamber and the sample capping layers are sputtered off. A high energy electron beam is focused onto the sample surface and the intensity and spin polarization of the emitted secondary electrons are measured, enabling simultaneous imaging of the topography and magnetization. Both orthogonal magnetization components within the plane of the sample are measured, so that the magnitude and direction of the in-plane magnetization are completely determined. The probing depth of the secondary electrons is limited to approximately 1 nm, making this technique a sensitive surface magnetometer.

SEMPA images for four of the disks are shown in Fig. 1. These are representative of the total of the disks imaged. Three of the disks present a nearly closed flux, four quadrant configuration typical of a system with cubic anisotropy. The magnetisation inside each quadrant domain is oriented along one of the $< 110 >$ directions, the easy magnetisation

axis of fcc Co(001). This is the prevalent state observed for the disks, but other magnetic configurations are also observed. In particular, the top right disk exhibits a magnetic state composed of two vortex cores with opposite orientations. As will be shown below, this can be understood in terms of the relaxation mechanism from saturation to remanence, where the two vortex cores become pinned, therefore inhibiting relaxation towards the equilibrium state. All of the disks have some net magnetic moment, since one of the domains is usually larger than the others (in particular, the vortex core does not sit exactly in the centre of the disk). The magnetization direction in this domain is the same as in the background film and in the direction along which the field was applied.

A higher magnification image of one of the disks, shown in Fig. 2, allows a closer look into the details of the four quadrant domain structure. In particular, an estimate of the width of the 90° domain wall can be obtained at this resolution. A domain wall profile between two domains in a similar disk is shown in Fig. 3. This line scan corresponds to the line drawn across the disk inset in the figure. We determine the domain wall width from the slope of the magnetization line scan at the middle of the domain wall ($\delta = \frac{\pi}{2}(\partial\theta/\partial x)_0^{-1}$) as shown in Fig. 2. For this wall, the measured width is 150 ± 25 nm. This is much wider than the value expected in bulk or continuous film systems.

In order to understand both the remanent magnetic states observed and the width of the domain wall, we performed micromagnetic simulations to first calculate the equilibrium state at remanence (starting from the saturated state along the magnetocrystalline easy axis direction), and second, to model the dynamics of the domain formation. The micromagnetic simulations were based on the OOMMF micromagnetic package.[23] The Co parameters used were $M_s = 1.424 \times 10^6$ A/m for the saturation magnetisation and $A = 3.3 \times 10^{-11}$ J/m for the exchange constant. The value of the anisotropy constant is crucial in determining the equilibrium state of the system. For fcc Co/Cu(001), the magnetic anisotropy has been estimated as $5 \pm 1 \times 10^4$ J/m^3,[18–20] not too dissimilar from the bulk value of 6×10^4 J/m^3.[24] In our simulations we used the experimental value[2] 6.5×10^4 J/m^3 and the thickness was set to 34 nm. The magnetization is assumed to be uniform in the vertical direction and a cell size of $(4\text{nm})^2$ is considered in the plane of the particle. For the present study, the magnetisation was first saturated along one magnetic easy axis and then was allowed to relax under no applied field. The equilibrium state at remanence as obtained from the micromagnetic simulations is shown in Fig. 4.

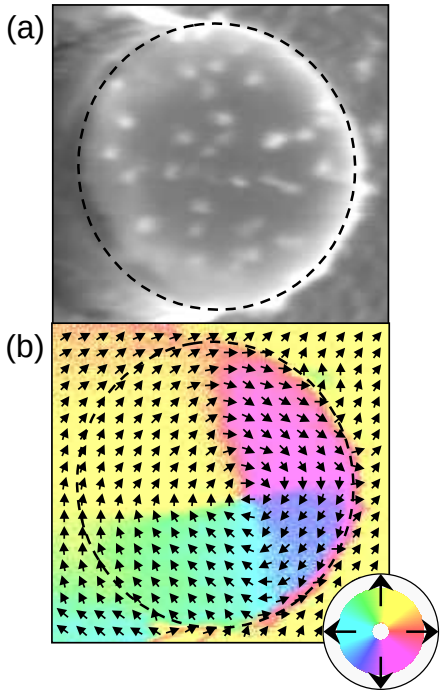

FIG. 2: SEMPA image of a disk with a quadrant state at higher magnification showing: (a) topography, and (b) magnetisation direction. The magnetisation direction is given both by colour, keyed to the inset colour wheel, and the superimposed arrow field.

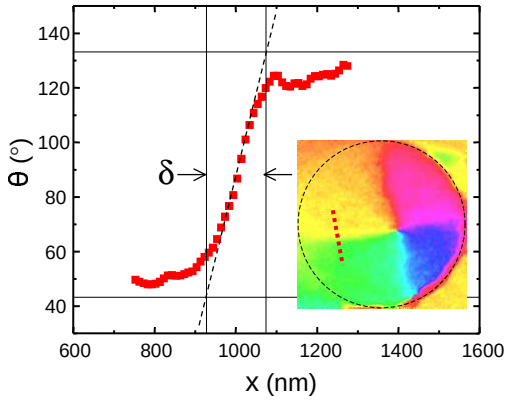

FIG. 3: Domain wall magnetisation profile between two domains.

The simulations show that, after saturation in an in-plane magnetic field, the dominant remanent equilibrium state is the quadrant state, as observed experimentally. The domain formation occurs by nucleation of two vortex cores on two opposite edges of the disk where the magnetostatic energy is maximum (i.e., at the ends of the dipole defined by the saturated state). The vortices need not occur simultaneously, and one may have a smaller nucleation

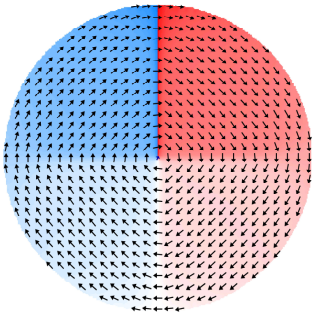

FIG. 4: Micromagnetic simulations for the remanent state after saturation.

energy and propagate throughout the disk, thus creating the quadrant state. When two vortices are created (as observed in our simulations), one of the vortices moves to the centre of the disk and pushes the other outwards until it vanishes. In some few instances, it may happen that these vortices are pinned by defects, and are still present in the remanent state as observed in some of the rings (top right disk of Fig. 1).

The domain wall magnetisation profile from the remanent state simulation is shown in Fig. 5. The width is the result of the energetic compromise between the exchange, anisotropy and dipolar interaction terms: while close to the perimeter of the disk the magnetisation minimises the free magnetic poles by remaining parallel to the perimeter, in the centre of the disk the spins try to orient along the magnetocrystalline easy axes. This results in a rather wide, geometrically constrained domain wall, whose width decreases from the outside towards the centre of the disk. In fact, we have calculated the domain wall width δ as a function of the normalised distance from the centre of the disk, r, to show how significant this variation is, Fig. 6. (The experimental data suggests that the variation of the domain wall width scales with the distance between the vortex core and the disk radius.) For small distances from the centre the DW width assumes a value close to $\frac{\pi}{2}(A/K)^{1/2}$ while at the periphery of the disk it assumes a value close to the geometrical parameter $r_0\pi/2$ corresponding to a circular magnetisation configuration (where r_0 is the disk radius). The situation in this case is analogous to the case of edge curling walls in patterned elements[25–27] and resembles also the equivalent in thick films of domain walls in closure domains,[28,29] where minimisation of the magnetic energy is achieved by extended domain walls that may reach the periphery of the element or the surface of the film, respectively. The experimental values show the same trend as the calculations, a plateau followed by an upturn in the domain width

with increasing distance from the vortex core, although the value of the domain wall at the plateau is a factor of two larger than that predicted by the simulations. This discrepancy may be due either to a smaller magnetocrystalline anisotropy constant than that measured in continuous films or to a larger exchange constant than that assumed in the calculations (or a combination of these two factors).

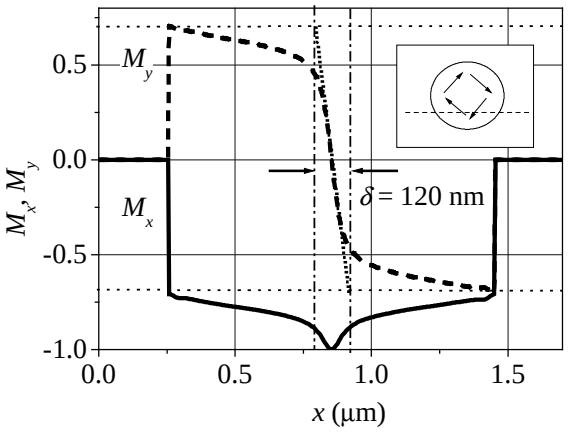

FIG. 5: Domain wall magnetisation profile between two domains as obtained from the micromagnetic simulations.

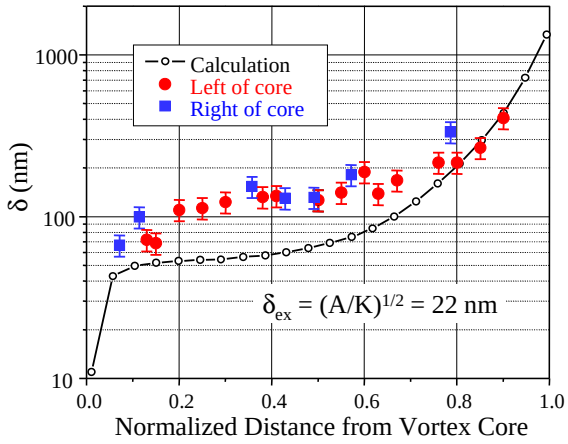

FIG. 6: Domain wall width as obtained from the calculated equilibrium configuration as a function of the distance from the centre of the disk.

III. CONCLUSIONS

In conclusion, we have studied the remanent magnetic configuration in fcc Co small disk elements. The prevalent state corresponds to a nearly closed flux, four quadrant configuration typical of systems with cubic anisotropy. Less frequently, other magnetic states may be stabilised by pinning sites for the domain wall during the transition from saturation to remanence. We show how the shape of the element combined with the cubic anisotropy energy term determines not only the equilibrium domain structure (quadrant state), but also gives rise to a geometrically constrained domain wall whose width increases with the distance from the vortex core. Both the observed remanent states and the measured width of the domain wall agree well with micromagnetic calculations, showing therefore that the observed domain wall structure is characteristic of small elements where the magnetocrystalline anisotropy strength is significant compared to the dipolar interaction.

Acknowledgments

This work was supported in part by the Office of Naval Research.

---

* Corresponding author; Electronic address: jacb1@phy.cam.ac.uk

[1] J.-G. Zhu, Y. Zheng, and G. A. Prinz, J. Appl. Phys. **87**, 6668 (2000).

[2] J. Rothman, M. Kläui, L. Lopez-Diaz, C. A. F. Vaz, A. Bleloch, J. A. C. Bland, Z. Cui, and R. Speaks, Phys. Rev. Lett. **86**, 1098 (2001).

[3] Y. Zheng and J.-G. Zhu, J. Appl. Phys. **81**, 5471 (1997).

[4] R. P. Cowburn, D. K. Koltsov, A. O. Adeyeye, M. E. Welland, and D. M. Tricker, Phys. Rev. Lett. **83**, 1042 (1999).

[5] G. Gubbiotti, L. Albani, G. Carlotti, M. D. Crescenzi, E. D. Fabrizio, A. Gerardino, O. Donzelli, F. Nizzoli, H. Koo, and R. D. Gomez, J. Appl. Phys. **87**, 5633 (2000).

[6] T. Pokhil, D. Song, and J. Nowak, J. Appl. Phys. **87**, 6319 (2000).

[7] T. Okuno, K. Shigeto, T. Ono, K. Mibu, and T. Shinjo, J. Magn. Magn. Mat. **240**, 1 (2002).

[8] J. M. García, A. Thiaville, J. Miltat, K. J. Kirk, J. N. Chapman, and F. Alouges, Appl. Phys. Lett. **79**, 656 (2001).

[9] M. Kläui, J. Rothman, L. Lopez-Diaz, C. A. F. Vaz, J. A. C. Bland, and Z. Cui, Appl. Phys. Lett. **78**, 3268 (2001).

[10] L. D. Buda, I. L. Prejbeanu, M. Demand, U. Ebels, and K. Ounadjela, IEEE Trans. Magn. **37**, 2061 (2001).

[11] R. Pulwey, M. Zölfl, G. Bayreuther, and D. Weiss, J. Appl. Phys. **91**, 7995 (2002).

[12] C. A. F. Vaz, L. Lopez-Diaz, M. Kläui, J. A. C. Bland, T. L. Monchesky, J. Unguris, and Z. Cui (46th Annual Conference on Magnetism and Magnetic Materials, Seattle, Washington, 2001), CD-15.

[13] M. Kläui, C. A. F. Vaz, J. A. C. Bland, T. L. Monchesky, J. Unguris, L. Heyderman, W. Wernsdorfer, and SPELEEM group, unpublished.

[14] P. Bruno, Phys. Rev. Lett **83**, 2425 (1999).

[15] S. P. Li, D. Peyrade, M. Natali, A. Lebib, Y. Chen, U. Ebels, L. D. Buda, and K. Ounadjela, Phys. Rev. Lett. **86**, 1102 (2001).

[16] C. A. F. Vaz and J. A. C. Bland, Phys. Rev. B **61**, 3098 (2000).

[17] R. Naik, C. Kota, J. S. Payson, and G. L. Dunifer, Phys. Rev. B **48**, 1008 (1993).

[18] M. Kowalewski, C. M. Schneider, and B. Heinrich, Phys. Rev. B **47**, 8748 (1993).

[19] B. Heinrich and J. F. Cochran, Adv. Phys. **42**, 523 (1993).

[20] B. Hillebrands, J. Fassbender, R. Jungleblut, G. Gunderot, D. Roberts, and G. Gehring, Phys. Rev. B **53**, R10548 (1996).

[21] M. Kläui, L. Lopez-Diaz, J. Rothman, C. A. F. Vaz, J. A. C. Bland, and Z. Cui, J. Magn. Magn. Mat. **240**, 7 (2002).

[22] M. R. Scheinfein, J. Unguris, M. H. Kelley, D. T. Pierce, and R. J. Celotta, Rev. Sci. Instrum. **61**, 2501 (1990).

[23] http://math.nist.gov/oommf.

[24] H. Fujiwara, H. Kadomatsu, and T. Tokunaga, J. Magn. Magn. Mater. **31-34**, 809 (1983).

[25] K. Yamamoto, H. Matsuyama, Y. Hamakawa, and M. Kitada, J. Appl. Phys. **75**, 2998 (1994).

[26] Y. Guo and J.-G. Zhu, J. Appl. Phys. **75**, 6388 (1994).

[27] R. Mattheis, K. Ramstöck, and J. McCord, IEEE Trans. Magn. **33**, 3993 (1997).

[28] A. Hubert and W. Rave, J. Magn. Magn. Mater. **196-197**, 325 (1999).

[29] A. Hubert and R. Schäfer, *Magnetic Domains* (Springer-Verlag, Berlin, 1998).